Matter and Radiation at Extremes | REVIEW | scitation.org/journal/mre

New opportunities for nuclear and atomic physics on the femto- to nanometer scale with ultra-high-intensity lasers

Cite as: Matter Radiat. Extremes 7, 024201 (2022); doi: 10.1063/5.0059405
Submitted: 9 June 2021 • Accepted: 16 November 2021 •
Published Online: 27 December 2021

View Online Export Citation CrossMark

Changbo Fu,[1,a)] Guoqiang Zhang,[2,b)] and Yugang Ma[1,c)]

AFFILIATIONS

[1] Key Laboratory of Nuclear Physics and Ion-Beam Application (MoE), Institute of Modern Physics, Fudan University, Shanghai 200433, China
[2] Shanghai Advanced Research Institute, Chinese Academy of Sciences, Shanghai 201210, China

Note: This paper is part of the Special Issue on Progress in Matter and Radiation at Extremes in China.
[a)] **Author to whom correspondence should be addressed:** cbfu@fudan.edu.cn
[b)] **Electronic mail:** zhangguoqiang@zjlab.org.cn
[c)] **Electronic mail:** mayugang@fudan.edu.cn

ABSTRACT

There are a number of puzzles concerning physics on the scale of nanometers to femtometers, including the neutron lifetime, the proton charge radius, and the possible existence of the deep Dirac level. With the development of high-intensity laser technology, lasers today can induce extremely strong electromagnetic fields. Electrons in the deep shells of atoms as well as the atomic nucleus itself can be affected by these fields. This may provide a new experimental platform for studies of physical processes on the femto- to nanometer scale, where atomic physics and nuclear physics coexist. In this paper, we review possible new opportunities for studying puzzles on the femto- to nanometer scale using high-intensity lasers.

I. INTRODUCTION

Atomic physics, which has a typical scale of nanometers, and nuclear physics, which has a typical scale of femtometers, have been studied for over a century. The α-particle backscattering experiment performed by Ernest Rutherford in 1909 led to the birth of the nuclear model of the atom,[1] which was a major step toward how we see the atom today: a nucleus with a diameter of the order of femtometers surrounded by an electron cloud with a diameter of the order of nanometer. It might appear as if, after more than 100 years, physical phenomena on the femto- to nanometer scale (FNMS) are well understood. However, the fact is that we are far from such a full understanding.

On the FNMS, the laws of both atomic physics and nuclear physics play important roles. On this scale, the forces involved are relatively simple compared with those in nuclei: beyond the nuclear surface, the influence of the strong force decreases very rapidly, and normally only the electromagnetic force governs the dynamics of electrons. However, in some cases, if a nucleus is radioactive, the weak force can also play an important role. In spite of the simple forces involved, on the FNMS, there are still many puzzling phenomena. These include the proton charge radius puzzle,[2] the neutron decay lifetime puzzle,[3,4] and the deep Dirac level puzzle.[5] Studies of these puzzles may lead to a deeper understanding of the structure of matter and may even reveal new physics beyond the Standard Model.

The development of high-intensity laser technology has provided a unique approach to the investigation of physics on the FNMS. Without any doubt, lasers are very useful tools for studying physics on very small spatial and temporal scales. One can deduce the structures of molecules and atoms by using narrowband lasers.[6] On very short timescales, one can deduce chemical bond dynamics by using picosecond and/or femtosecond lasers.[7] Because of their enveloping electron clouds, nuclei are well shielded and have not been thoroughly studied. With high-intensity lasers, however, atoms can become highly ionized, and nuclei then become important. Despite this, the new opportunities on the FNMS presented by the availability of such lasers, connecting atomic physics nuclear physics, have not yet been fully exploited.

In this paper, we will first review several puzzles that exist on the FNMS. We will then review several theoretical tools that can be applied on the FNMS to analyze many-body systems involving photons (lasers), electrons, and nuclei. Applications, including nuclear clocks and nuclear batteries, will also be discussed.

II. PUZZLES ON THE FNMS

A. Neutron lifetime

A free neutron will decay into a proton, electron, and antineutrino through the weak interaction, $n \to p + e + \bar{\nu}_e$. The neutron decay lifetime is very important in fields such as particle physics and astrophysics.[8] In particle physics, the neutron lifetime plays a critical role in determining basic parameters such as the quark mixing angles, quark coupling constants, and cross sections related to weak p–n interactions.[9,10] In nuclear astrophysics, the neutron lifetime determines the speed of nucleosynthesis in the Big Bang and in the stars. In the first few seconds after the Big Bang, protons and neutrons were formed. A few minutes later, as the universe expanded, its temperature dropped below the photodissociation threshold for deuterons, the equilibrium ratio of protons and neutrons was broken, and primordial nucleosynthesis started. A precise value of the neutron lifetime is an important input parameter for calculations of primordial nucleosynthesis.

It is very interesting that a consistent experimental value of the neutron lifetime has yet to be obtained. Different values have been found by different groups using different techniques.

Two major types of experiments have been performed to measure the neutron lifetime: beam experiments, which use neutron fluxes, and bottle experiments, which use ultra-cold neutrons confined in containers.[3,4] After many years of effort, the neutron lifetime measured with the beam method is (888.1 ± 2.0) s, while with the bottle method it is (879.45 ± 0.58) s.[11] The difference between the averages from the two methods is (8.7 ± 2.1) s, which is 4.1σ. This persistent disagreement may be related to an unknown process in neutron decay, or even to physics beyond the Standard Model.

The neutron decay $n \to p + e + \bar{\nu}_e$ involves the weak interaction, and the weak interaction has effects both on the nuclear scale and on the atomic scale, in other words, the FNMS. Therefore, a deeper study on the FNMS might help to resolve the neutron lifetime puzzle.

B. Deep Dirac level

The so-called deep Dirac level (DDL) is another very interesting puzzle arising on the FNMS. The history of the DDL can be traced back to the time when the Dirac equation was first established. As is now well known, one "unphysical" solution was interpreted as corresponding to the positron. In fact, there is another "unphysical" solution, namely, the DDL, which is not so well known and has generally been rejected as having no physical significance. However, it has attracted some attention over the years, and claims have been made that the DDL, like the "unphysical" solution corresponding to the positron, may indeed be related to a physical state.

The Dirac equation for an electron moving around a nucleus can be written as[12]

$$[\alpha \cdot \boldsymbol{p} + \beta M + V(r)]\boldsymbol{\Psi} = E\boldsymbol{\Psi}. \tag{1}$$

Here, the Dirac matrices are

$$\alpha = \begin{pmatrix} 0 & \boldsymbol{\sigma} \\ \boldsymbol{\sigma} & 0 \end{pmatrix}, \quad \beta = \begin{pmatrix} I & 0 \\ 0 & -I \end{pmatrix}, \tag{2}$$

where $\boldsymbol{\sigma}$ is the Pauli matrix and I the unit matrix, and $V(r) = -Z\alpha\hbar c/r$ is the Coulomb potential, where α is the fine structure constant, r is the distance between the electron and the nucleus, and Z is the charge of the nucleus. The Dirac equation (1) has the solution

$$\boldsymbol{\Psi} = \begin{pmatrix} g(r)\Omega_{jlm}(\theta,\phi) \\ \mathrm{i}f(r)\Omega_{j\bar{l}m}(\theta,\phi) \end{pmatrix}, \quad j = l \pm \frac{1}{2}, \quad l + \bar{l} = 2j, \tag{3}$$

where Ω_{jlm} are two-component angular momentum spinors. With the ansatz $f \propto r^{\gamma}$ and $g \propto r^{\gamma}$, one has[1]

$$\gamma = \pm\sqrt{\left(j+\frac{1}{2}\right)^2 - Z^2\alpha^2}. \tag{4}$$

It is argued that the expectation value of the Coulomb energy is given by

$$\begin{aligned} E_C &= \int \boldsymbol{\Psi}^{\dagger}\left(-\frac{Ze^2}{r}\right)\boldsymbol{\Psi}\,\mathrm{d}^3r \\ &= \int (f^2+g^2)\left(-\frac{Ze^2}{r}\right)\mathrm{d}^3r \\ &\propto \int r^{2\gamma}\left(-\frac{Ze^2}{r}\right)\mathrm{d}^3r. \end{aligned} \tag{5}$$

For negative γ, one has $E_C|_{\gamma<-1/2} \to \infty$, which is unphysical. However, this infinity comes from the point-like potential $V(r) = -Z\alpha\hbar c/r$, i.e., the assumption that the nucleus is a point charge. If instead it is assumed that the nucleus has a finite charge radius, the singularity is removed, and E_C is finite too. The problem then becomes one of matching the solutions inside and outside the nucleus on the surface of the nucleus.[13]

One can see the unconventional solution more clearly from the Klein–Gordon equation. It is well known that the Dirac equation can be transformed into the Klein–Gordon equation by taking the squares of both sides of Eq. (1),

$$\{\nabla^2 + [V(r) - \mathrm{i}\hbar\partial_t]^2 - M^2\}\boldsymbol{\Psi} = 0. \tag{6}$$

In spherical coordinates, this can be written as

$$\begin{aligned} &\left[\frac{1}{r}\frac{\partial}{\partial r}\left(r^2\frac{\partial}{\partial r}\right) + \frac{1}{r^2\sin\theta}\frac{\partial}{\partial\theta}\left(\sin\theta\frac{\partial}{\partial\theta}\right)\right. \\ &\left.\quad + \frac{1}{r^2\sin^2\theta}\frac{\partial^2}{\partial\phi^2} + (\mathrm{i}\hbar\partial_t - V)^2 - M^2\right]\psi(r,\theta,\phi) = 0. \end{aligned} \tag{7}$$

The total wave function $\psi(r, \theta, \phi, t)$ can be written as

$$\psi(r,\theta,\phi,t) = \frac{R(r,t)}{r}Y_{lm}(\theta,\phi) = \frac{R(r,t)}{r}\Theta(\theta)\Phi(\phi). \tag{8}$$

Here, $R(r, t)$, $\Theta(\theta)$, and $\Phi(\phi)$ are solutions of the equations

$$\left[\frac{\mathrm{d}^2}{\mathrm{d}r^2} + (\mathrm{i}\hbar\partial_t - V)^2 - M^2 - \frac{l(l+1)}{r^2}\right]R(r,t) = 0, \tag{9a}$$

$$\frac{\mathrm{d}^2\Theta(\theta)}{\mathrm{d}\theta^2} + \cot\theta\frac{\mathrm{d}\Theta(\theta)}{\mathrm{d}\theta}\left[l(l+1) - \frac{m^2}{\sin^2\theta}\right]\Theta(\theta) = 0, \tag{9b}$$

$$\frac{\mathrm{d}^2\Phi(\phi)}{\mathrm{d}\phi^2} + m^2\Phi(\phi) \quad = 0. \tag{9c}$$

In the case $l = 0$, Eq. (9a) has the solution[14]

$$R(r,t) = \frac{r_0^{-\gamma/2-1} r^{(\gamma-1)/2} \mathrm{e}^{-r/r_0}}{2^{-\gamma/2}\sqrt{\pi\Gamma(\gamma+2)}} \mathrm{e}^{-\mathrm{i}E_0 t/\hbar}, \tag{10}$$

where $\Gamma(x)$ is the gamma function and

$$E_0 = m_0c^2\frac{Z\alpha}{\sqrt{(1-\gamma)/2}}, \qquad r_0 = \frac{\hbar}{m_0c}\frac{1}{\sqrt{(1-\gamma)/2}}. \tag{11}$$

As in the case of the Dirac equation, the negative-branch $\gamma = -\sqrt{1-4Z^2\alpha^2}$ solution is the "unphysical" one.[1] The energy, orbit, and wave function can be simplified as

$$E_0^\# = m_0c^2 Z\alpha \simeq m_0c^2 - (511 - 3.72Z)\ \mathrm{keV}, \tag{12}$$

$$r_0^\# \simeq \frac{\hbar}{m_0c} \simeq 0.003\,9\,\text{Å}, \tag{13}$$

$$R^\#(r,t) \simeq \frac{r^{-1}\mathrm{e}^{-r/r_0^\#}}{\sqrt{2\pi r_0^\#}} \mathrm{e}^{-\mathrm{i}E_0^\# t/\hbar}. \tag{14}$$

It can be seen that $\lim_{r\to 0} R^\# = \infty$. However, the singularity can be removed if the nucleus is not assumed to be a point-like particle as described by the potential $V(r) = -Z\alpha\hbar c/r$. The wave function itself is also square-integrable, i.e., $\int|\Psi|^2\mathrm{d}^3r = 1$. Furthermore, one can check that E_C in Eq. (5) is also finite if Eqs. (8) and (14) are substituted into it.

It is worth noting that a solution of a Klein–Gordon equation is not automatically a solution of the corresponding Dirac equation. An experimental discovery of an electron state corresponding to the Klein–Gordon equation but not to the Dirac equation might give a hint that under symmetry breaking, an electron is intermediate between a fermion and a boson.

The existence of the DDL has been a subject of theoretical debate, and there have been claims that the DDL is responsible for some experimentally observed phenomena,[15–17] although these claims have been questioned.[18–22] New sensitive experimental detection methods are needed.

As one can see, taking $Z = 1$ as an example, in the case of the DDL, the electron is deeply bound, with an energy of 0.5073 MeV, compared with the well-known Bohr ground-state value of 13.6 eV. The orbit of the DDL is only about 390 fm from the nucleus, compared with the Bohr ground-state orbit of 0.53 Å (5.3×10^4 fm). In Ref. 5, the authors proposed the electron capture lifetime as a novel indicator of the existence of the DDL. Because the DDL orbit is so close to the nucleus, the probability of the electron being captured is dramatically enhanced.

C. Proton charge diameter

Neutrons and protons are fundamental building blocks of the visible matter around us. However, despite the many years that have passed since their discovery (that of the proton being credited to Rutherford in 1917 and that of the neutron to Chadwick in 1932), our knowledge of some basic physical quantities related to these particles is still incomplete. Measurements of the proton charge radius have been carried out since the 1950s,[2,23] but some mysteries remain with regard to this quantity.

The proton charge radius can be determined using two main experimental techniques: electron–proton (e–p) elastic scattering, and high-resolution spectroscopy of electronic and muonic hydrogen atoms. These different techniques result in conflicting values for the proton charge radius. Over ten different electronic transitions have been measured in electronic hydrogen, as well as in muonic hydrogen,[2] and most electronic hydrogen results are compatible with the muonic hydrogen ones within 1.5σ. However, in the case of e–p elastic scattering, the results from different groups differ by as much as 5σ.[2] This conflict represents a major problem in proton structure physics. Its resolution may lead to new discoveries concerning proton and hydrogen atom structure on the FNMS.

To resolve the disagreement between the various results, a better understanding may be needed of the structure on the FNMS. For example, if the DDL exists, the two processes of the e–p scattering and the Lamb shift of the hydrogen atom could give different results for the proton charge radius. On the one hand, a precise value for this radius would provide input to help solve other puzzles on the FNMS; on the other hand, new structures such as the DDL might help to resolve the proton size puzzle.

III. MECHANISMS ON THE FNMS

A. NEEC and NEET

Internal conversion is a well-known nuclear decay process. An excited nucleus may kick off an electron from the ith atomic shell with branching ratio κ_i, or a γ photon with branching ratio κ_γ. The internal conversion coefficient α_T is defined as[24]

$$\alpha_T = \sum_i \alpha_i = \sum_i \frac{\kappa_i}{\kappa_\gamma}. \tag{15}$$

For many nuclear isomers, α_T is much larger than 1, which means that it is very difficult for the nucleus to decay through the channel $N^* \to N + \gamma$, and the channel $N^* \to N + e$ is preferred. Therefore, for

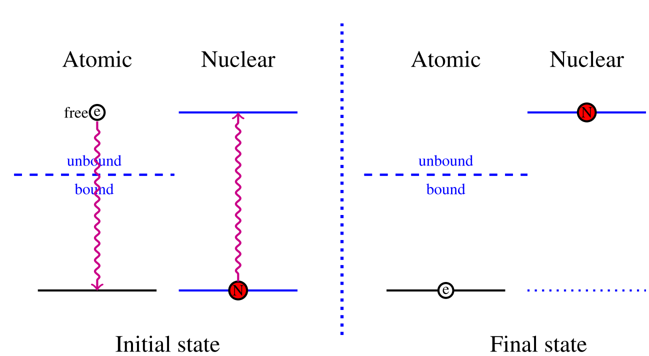

FIG. 1. Atomic and nuclear states involved in a NEEC transition. Initially, the electron is unbound and the nucleus is in its ground state, whereas in the final state, the electron is bound and the nucleus is excited to a higher-energy state.

an $\alpha_T \gg 1$ nucleus N, the inverse process $e + N \to N^*$ is a much more efficient way to excite N than $\gamma + N \to N^*$. If initially the electron is free and then becomes bound to the atom (Fig. 1),

$$N + e^{(\text{free})} \to N^* + e^{(\text{bound})}, \tag{16}$$

the process is called nuclear excitation by electron capture (NEEC).[25,26] If initially the electron is bound and then moves to a deeper atomic level (Fig. 2),

$$N + e^{(\text{bound 1})} \to N^* + e^{(\text{bound 2})}, \tag{17}$$

the process is called nuclear excitation by electron transfer (NEET).[27–30]

The NEEC process was first proposed by Goldanskii and Namiot.[31] Based on Fermi's golden rule, one may write the NEEC cross section as[25,26,32]

$$\sigma_{\text{NEEC}}(E) = \frac{(2\pi\hbar)^2}{2m_e E}\frac{2J_f + 1}{2J_i + 1}\Gamma^e_{J_i \to J_f}\frac{\Gamma^{\text{tot}}}{(E - E_r)^2 + (\Gamma^{\text{tot}}/2)^2}, \tag{18}$$

where m_e is the electron mass, J_i and J_f are the initial and final nuclear spins, Γ^{tot} is the total transition width, $\Gamma^e_{J_i \to J_f}$ is the transition width of $J_i \to J_f$, E is the energy, and E_r is the resonance energy.

The NEET process was first proposed by Morita and Otozai.[30] In the weak-coupling limit ($\kappa \to 0$), the NEET cross section can be written as[28]

$$\sigma^{\kappa\to 0}_{\text{NEET}} = \frac{\Gamma_i \Gamma_f}{\Gamma_i}\frac{\kappa^2}{(E_i - E_f)^2 + (\Gamma^{\text{tot}}/2)^2}, \tag{19}$$

where $\kappa = \langle f|i\rangle$, with i and f representing the initial and final states, Γ is the transition width, and E is the binding energy.

In a laser–plasma environment, where there are a lot of energetic electrons, NEEC and NEET may dominate the generation of nuclear isomers through the reactions shown in Eqs. (16) and (17).

B. Electron bridge

As with the NEET and NEEC processes, the electron bridge (EB) process can be the dominant channel for a nuclear isomer that has a resonance channel available[33,34]

The EB process is shown in Fig. 3. Initially, the electron involved is in a lower bound state with energy E_{e0}, and the nucleus is in the ground state. The electron may absorb one or even two photons with energies E_{p1} (and E_{p2} if two photons are absorbed) and jump to a

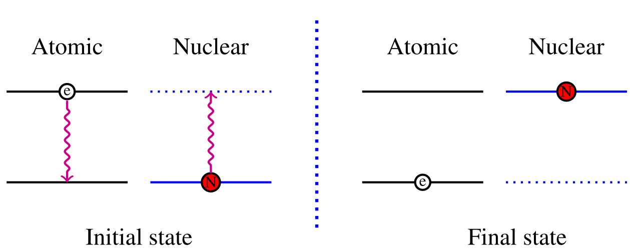

FIG. 2. Atomic and nuclear states involved in a NEET transition. Initially, the electron is in a bound excited state and the nucleus is in the ground state, whereas in the final state, the electron is in a lower-energy bound state and the nucleus is in an excited state.

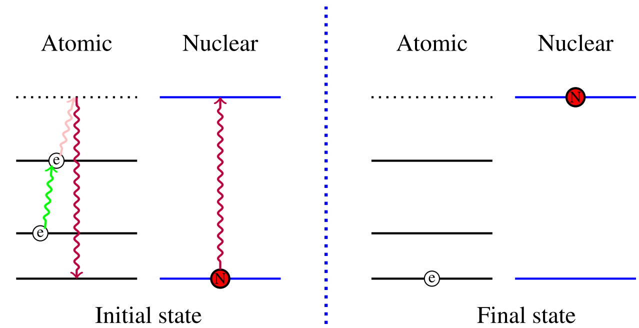

FIG. 3. Atomic and nuclear states involved in an EB transition. Initially, the electron is in a bound state and the nucleus is in the ground state. When the electron absorbs a photon (pink line) or two photons (green + pink lines), it is excited to a virtual higher state. The electron may then drop to the ground state, while at the same time the nucleus is excited to a higher-energy state.

virtual state E_e^*. If $E_{e0} + E_{p1} + E_{p2} = E_e^* = E_m$, where E_m is the excited energy of the nuclear isomer, the nucleus can jump up to the corresponding isomeric state resonantly.

The EB process has the following advantages. First, it enables the study of isomers with relatively large E_m. At present, optical lasers with photon energies E_p higher than tens of electron volts are not available. Free-electron lasers (FELs) may have higher photon energies, but also have much larger bandwidths.[35] Thus, by choosing an appropriate $\Delta E = E_{p1} + E_{p2}$, one can study isomers with higher E_m. Second, the EB process can greatly improve the photon absorption cross section. In fact, even if one has a laser with a photon energy $E_p = E_m$, the photon absorption cross section σ_γ of the reaction $\gamma + X \to X^{(*)}$ is still very small, mainly because of the very small nuclear diameter. However, with the EB mechanism, the enhancement factor can be increased by a factor of between 10 and 10^9.[36,37] The enhancement factor for a single EB can be written as[36]

$$R_{\text{EB}} \equiv \frac{\sigma_{\text{EB}}}{\sigma_\gamma} \propto \frac{\Gamma_{\text{EB}}\Gamma_l^2}{\Gamma_\gamma}, \tag{20}$$

where σ_{EB} is the cross section through the EB mechanism, Γ_l is the linewidth of the laser, Γ_{EB} is the nuclear EB-decay channel width, and Γ_γ is the nuclear γ-decay channel width. For the two-photon EB, the dependence is similar to that in the one-photon case.[37]

IV. POTENTIAL APPLICATIONS RELATED TO THE FNMS

A. Nuclear clocks

Clocks are fundamental devices for physics: without precise clocks, there would be no modern physics. From ancient sundials and sandglasses to modern atomic clocks, clocks have become more and more accurate, and the search goes on for ever more precision. In 2019, scientists from the National Institute of Standards and Technology (NIST) demonstrated an Al^+ clock with a total uncertainty of 9.4×10^{-19} s.[38]

Normally, a nuclear transition has a much smaller $\Delta E/E$, where ΔE is the spectral linewidth and E is the energy difference of the transition. A smaller $\Delta E/E$ means a more accurate clock.[39] Recently, a transition in cesium atoms was found to have an uncertainty of 2.5×10^{-19} s.[40] However, it has become more and more difficult to find a transition with an uncertainty smaller than the order of 10^{-19} s in atoms. However, in nuclear isotopes, there are many transitions for which $\Delta E/E$ is much smaller than in atoms, and it is expected that the exploitation of nuclear transitions will lead to a new generation of clocks, namely, nuclear clocks (or gamma clocks).

There are two nuclear isomers, ^{229m}Th and ^{235m}U, that appear to be particularly promising for producing a nuclear clock. The isomer ^{229m}Th has an excited energy of (8.10 ± 0.17) eV,[41–44] while ^{235m}U has a higher excited energy of 76 eV.[45] These energies are relatively low and are reachable using current optical laser technology.

The ability to excite nuclei to their isomer states is the precondition for making a nuclear clock. Limitations of laser technology mean that lasers with appropriate wavelengths and precision to match the isomeric energies are not currently available, and so indirect excitation schemes such as NEEC, NEET, and EB are being investigated as alternatives.

B. Nuclear batteries

Physics on the FNMS has another application, namely, in nuclear batteries. Owing to their long lifetime, environmental stability, and high energy density, nuclear batteries have been widely used in aerospace, deep-sea and polar exploration, cardiac pacemakers, and micro electric motors, among other applications.[46,47] Many radioactive materials can be used in nuclear batteries, including those subject to α, β, or γ decay. Nuclear isomers are among these and have advantages such as the ability to be recharged. In particular, ^{93m}Mo, ^{180m}Ta, and ^{178m}Hf are candidates for use in nuclear batteries. The processes of NEET, NEEC, and EB may be used to enhance production rates.

V. HIGH-INTENSITY LASERS AND THE FNMS

High-intensity laser facilities provide new opportunities to study various physical processes happening on the FNMS, especially nonlinear processes.

Most of the nucleus–laser interactions achievable with today's laser techniques are indirect. The current record laser intensity[48] is 1.1×10^{23} W/cm^2. The electric field of a laser can be written in terms of its intensity I as

$$\mathbf{E} = 27.4 \times \left(\frac{I}{[\mathrm{W/cm^2}]}\right)^{1/2} \ [\mathrm{V/cm}]. \tag{21}$$

As a classic limiting estimate, the Hamiltonian of nucleons (specifically protons) in the nucleus has an extra term $\Delta H = e\sum_i \phi_i(t)$, where ϕ_i is the potential of the ith proton in the laser field. The order of magnitude of the average potential $\langle \Delta H \rangle$ can be estimated to be

$$\Delta H = O(De\mathbf{E}), \tag{22}$$

where D is the nuclear diameter and e is the electron charge. If take $I = 10^{23}$ W/cm^2 and $D = 10$ fm, then we have $\Delta H \approx 10$ eV. One can see that low-lying levels like those in ^{229}Th (8.1 eV) and ^{235}U (74 eV) might possibly be excited directly by the strongest laser currently available. In fact, this estimate is only an upper limit, and recently Au ions with charge states up to 72+ have been observed using lasers with intensity of the order of 10^{22} W/cm^2.[49,50] It is still very difficult in practice to fully strip electrons from a nucleus, and if the electrons are not fully stripped, then the electric field in Eq. (22) will be weakened by the electron cloud. Furthermore, most nuclear excited states are in the keV and MeV ranges. Therefore, until the Schwinger limit,[51] corresponding to 2.3×10^{29} W/cm^2 (or $E = 1.3 \times 10^{16}$ V/cm), can be achieved, it will not be possible for most nuclear isotopes to be excited directly by lasers.

Indirect nucleus–laser interaction could be huge owing to the resonance mechanisms involved in NEEC, NEET, and EB. For the NEEC and NEET processes, electrons with energy of the order of keV are needed. One can estimate the order of magnitude of the electron energy using a formula similar to Eq. (22):

$$\mathcal{E}_e = O(\lambda e\mathbf{E}), \tag{23}$$

where λ is the laser wavelength. The physical meaning of $\mathcal{E}_e$ is the order of magnitude of the energy of one electron driven by a laser during one cycle of the laser's electromagnetic field oscillation. In fact, in a typical high-intensity laser experiment, the electron temperature can easily reach the keV level.[52] At the same time, atoms are ionized to high charge states. Therefore, a laser-induced plasma is an ideal platform for studies of NEEC and NEET.[53,54]

Furthermore, as shown in Eqs. (18)–(20), NEEC, NEET, and EB processes are highly dependent on the nuclear decay width. In a plasma or in high-intensity laser fields, without the shielding from the electron cloud, the nuclei can experience a relatively strong time-dependent potential $\Delta V(t)$. This extra $\Delta V(t)$ may broaden the bound-state width. Considering the fact that many nuclear isomers have energy widths that are much smaller than an electron volt, an eV-level extra potential $\Delta V(t)$, as estimated by Eq. (22), could dramatically improve absorption widths.

Normally, for the EB process, narrowband photon sources are needed. However, in a laser-induced plasma, the atomic, as well as nuclear, absorption lines are broadened owing to the Doppler effect.[55–58] Furthermore, one nonlinear process, namely, the surface enhancement effect,[59] may also be used to enhance the EB effect when a high-intensity laser is used. It is well known that with surface-enhanced Raman scattering, Raman spectra have a sensitivity that is improved by a factor of more than 10^{10} compared with ordinary ones, enabling the detection of single molecules.[6] This nonlinear effect can also improve the NEEC, NEET, and EB processes in laser-induced plasmas.

To observe the NEEC, NEET, and EB processes in laser-induced plasmas experimentally, the nuclear isomers to be studied, as well as the intensities of the inducing lasers, need to be chosen carefully. As discussed earlier, experimental observation of the NEEC, NEET, or EB processes will be easier for isomers with internal conversion coefficient $\alpha_T \gg 1$. It is well known that internal conversion coefficients α_T are energy-dependent and atomic-shell-dependent.[24] For example, in the case of a $Z = 10$ nucleus, for the $E3$ transition, with γ energy $E_\gamma = 1.5$ keV, the internal conversion coefficient of the K shell can be as high as $\alpha_K = 4 \times 10^7$, while that of the L_3 shell is only about $\alpha_{L_3} = 18$. Therefore, if the temperature of a laser-induced plasma is not high enough, the electrons occupying the corresponding shell cannot be excited, and one cannot then observe the expected processes. For different atoms, the charge states can be different. The plasma temperature depends on the intensity of the inducing laser and the nature of the target structure (e.g., its thickness and whether it is in the form of a foam or nanowires). Therefore, the appropriate intensity of the lasers that is used to induce the plasma can also differ. Today, lasers with relativistic strength are widely available. Atoms can be excited to charge states over 20+ with modern lasers.

Furthermore, relativistic lasers can trigger the $\gamma \to e^+ + e^-$ reaction, which may offer a way to investigate the existence of the DDL. Once an e^+e^- pair has been produced, the e^- may remain in the DDL orbit. If the nucleus is in an excited state, specifically a nuclear isomer state, and decays through orbital electron capture, the decay lifetime of the nucleus could then be dramatically different, given that an electron in the DDL is much closer to the nucleus than one in the K shell or another atomic shell. The closer an electron is to the nucleus, the more easily will it be captured. It is estimated that the lifetime of an electron in the DDL will be reduced by a factor of 1000.[5] The discoveries of new structures at the atomic level may help to solve the neutron lifetime and proton charge radius puzzles.

VI. SUMMARY

We have reviewed some puzzles that may be related to the FNMS. These concern the possible existence of the so-called deep Dirac level, the neutron lifetime, and the proton size. It is suspected that there may be some as-yet unknown physical processes that occur on the FNMS. We have also reviewed the mechanisms linking nuclear decays to atomic structures, namely, NEEC, NEET, and the EB process. For an excited nucleus with β-related decay channels, the nucleus and the electrons interact via the weak force, and NEEC, NEET, and the EB process can be used to investigate the resulting behavior. From an experimental point of view, currently available high-intensity lasers are still not strong enough to have a direct effect on nucleons in the nucleus. However, they will have direct effects on the electrons bound to a nucleus. Given the role of electrons in the weak interaction, high-intensity laser facilities may play a critical role in studies of the puzzles on the FNMS.

ACKNOWLEDGMENTS

This work is supported by the National Nature Science Foundation of China (Grant No. 11875191) and the Strategic Priority Research Program of the Chinese Academy of Sciences (Grant No. XDB16).

AUTHOR DECLARATIONS

Conflict of Interest

The authors declare no competing financial interests.

DATA AVAILABILITY

All of the relevant data that support the findings of this study are available from the corresponding authors upon reasonable request.

REFERENCES

[1] L. I. Schiff, *Quantum Mechanics*, 3rd ed. (McGraw-Hill Publishing Company, New York, 1968).

[2] J.-P. Karr, D. Marchand, and E. Voutier, "The proton size," Nat. Rev. Phys. **2**, 601–614 (2020).

[3] A. T. Yue, M. S. Dewey, D. M. Gilliam, G. L. Greene, A. B. Laptev, J. S. Nico, W. M. Snow, and F. E. Wietfeldt, "Improved determination of the neutron lifetime," Phys. Rev. Lett. **111**, 222501 (2013).

[4] F. E. Wietfeldt and G. L. Greene, "Colloquium: The neutron lifetime," Rev. Mod. Phys. **83**, 1173–1192 (2011).

[5] C. Fu, X. Zhang, and D. Dechang, "Feasibility study on the deep Dirac levels with high-intensity lasers," Nucl. Phys. Rev. **37**, 377–381 (2020).

[6] K. Kneipp, Y. Wang, H. Kneipp, L. T. Perelman, I. Itzkan, R. R. Dasari, and M. S. Feld, "Single molecule detection using surface-enhanced Raman scattering (SERS)," Phys. Rev. Lett. **78**, 1667–1670 (1997).

[7] K. C. Harper, E. G. Moschetta, S. V. Bordawekar, and S. J. Wittenberger, "A laser driven flow chemistry platform for scaling photochemical reactions with visible light," ACS Cent. Sci. **5**, 109–115 (2019).

[8] B. D. Fields, K. A. Olive, T.-H. Yeh, and C. Young, "Big-bang nucleosynthesis after Planck," J. Cosmol. Astropart. Phys. **80**, 543 (2020).

[9] S. Paul, "The puzzle of neutron lifetime," Nucl. Instrum. Methods Phys. Res., Sect. A **611**, 157–166 (2009).

[10] W.-B. Ding, Z. Yu, Y. Xu, C.-J. Liu, and T. Bao, "Neutrino emission and cooling of dark-matter-admixed neutron stars," Chin. Phys. Lett. **36**, 049701 (2019).

[11] F. E. Wietfeldt, "Measurements of the neutron lifetime," Atoms **6**, 70 (2018).

[12] B. Goodman and S. R. Ignjatović, "A simpler solution of the Dirac equation in a Coulomb potential," Am. J. Phys. **65**, 214–221 (1997).

[13] W. Greiner, *Relativistic Quantum Mechanics*, 3rd ed. (Springer-Verlag Berling Heidelberg, New York, 2000).

[14] J. Naudts, "On the hydrino state of the relativistic hydrogen atom," arXiv:physics/0507193 (2005).

[15] J. Phillips, R. L. Mills, and X. Chen, "Water bath calorimetric study of excess heat generation in 'resonant transfer' plasmas," J. Appl. Phys. **96**, 3095–3102 (2004).

[16] R. Mills and P. Ray, "Extreme ultraviolet spectroscopy of helium–hydrogen plasma," J. Phys. D: Appl. Phys. **36**, 1535 (2003).

[17] J. Va'vra, "A new way to explain the 511 keV signal from the center of the galaxy and some dark matter experiments," arXiv:1304.0833 (2013).

[18] S. Jovićević, N. Sakan, M. Ivković, and N. Konjević, "Spectroscopic study of hydrogen Balmer lines in a microwave-induced discharge," J. Appl. Phys. **105**, 013306 (2009).

[19] A. Rathke, "A critical analysis of the hydrino model," New J. Phys. **7**, 127 (2005).

[20] A. Phelps, "Comment on 'Water bath calorimetric study of excess heat generation in resonant transfer plasmas,," J. Appl. Phys. **96**, 066108 (2005).

[21] N. Dombey, "The hydrino and other unlikely states," Phys. Lett. A **360**, 62–65 (2006).

[22] A. S. de Castro, "Orthogonality criterion for banishing hydrino states from standard quantum mechanics," Phys. Lett. A **369**, 380–383 (2007).

[23] R. Pohl, A. Antognini, F. Nez, F. D. Amaro, F. Biraben, J. M. R. Cardoso, D. S. Covita, A. Dax, S. Dhawan, L. M. P. Fernandes, A. Giesen, T. Graf, T. W. Hänsch, P. Indelicato, L. Julien, C.-Y. Kao, P. Knowles, E.-O. Le Bigot, Y.-W. Liu, J. A. M. Lopes, L. Ludhova, C. M. B. Monteiro, F. Mulhauser, T. Nebel, P. Rabinowitz, J. M. F. dos Santos, L. A. Schaller, K. Schuhmann, C. Schwob, D. Taqqu, J. F. C. A. Veloso, and F. Kottmann, "The size of the proton," Nature **466**, 213–216 (2010).

[24] I. M. Band, M. B. Trzhaskovskaya, C. W. Nestor, JR, P. O. Tikkanen, and S. Raman, "Dirac–Fock internal conversion coefficients," At. Data Nucl. Data Tables **81**, 1–334 (2002).

[25] A. Pálffy, W. Scheid, and Z. Harman, "Theory of nuclear excitation by electron capture for heavy ions," Phys. Rev. A **73**, 012715 (2006).

[26] A. Pálffy, Z. Harman, and W. Scheid, "Quantum interference between nuclear excitation by electron capture and radiative recombination," Phys. Rev. A **75**, 012709 (2007).

[27] S. Kishimoto, Y. Yoda, M. Seto, Y. Kobayashi, S. Kitao, R. Haruki, T. Kawauchi, K. Fukutani, and T. Okano, "Observation of nuclear excitation by electron transition in ^{197}Au with synchrotron x rays and an avalanche photodiode," Phys. Rev. Lett. **85**, 1831–1834 (2000).

[28] I. Ahmad, R. W. Dunford, H. Esbensen, D. S. Gemmell, E. P. Kanter, U. Rütt, and S. H. Southworth, "Nuclear excitation by electronic transition in ^{189}Os," Phys. Rev. C **61**, 051304 (2000).

[29] P. Morel, J. M. Daugas, G. Gosselin, V. Méot, and D. Gogny, "Nuclear excitation by electronic processes: NEEC and NEET effects," Nucl. Phys. A **746**, 608–612 (2004).

[30] M. Morita and K. Otozai, "Theory of nuclear excitation by electron transition (NEET) and experimental evidence in ^{189}Os and ^{237}Np," Hyperfine Interact. **2**, 418 (1976).

[31]V. I. Goldanskii and V. A. Namiot, "On the excitation of isomeric nuclear levels by laser radiation through inverse internal electron conversion," Phys. Lett. B **62**, 393 (1976).
[32]P. Morel, J. M. Daugas, G. Gosselin, V. Méot, and D. Gogny, "Nuclear excitation by electronic processes: NEEC and NEET effects," AIP Conf. Proc. **769**, 1085–1088 (2005).
[33]V. A. Krutov and V. N. Fomenko, "Influence of electronic shell on gamma radiation of atomic nuclei," Annalen der Physik **21**, 291 (1968).
[34]P. V. Bilous, H. Bekker, J. C. Berengut, B. Seiferle, L. von der Wense, P. G. Thirolf, T. Pfeifer, J. R. C. López-Urrutia, and A. Pálffy, "Electronic bridge excitation in highly charged ^{229}Th ions," Phys. Rev. Lett. **124**, 192502 (2020).
[35]B. W. J. McNeil and N. R. Thompson, "X-ray free-electron lasers," Nat. Photonics **4**, 814 (2010).
[36]L. von der Wense, and B. Seiferle, "The ^{229}Th isomer: Prospects for a nuclear optical clock," Eur. Phys. J. A **56**, 277 (2020).
[37]N.-Q. Cai, G.-Q. Zhang, C.-B. Fu, and Y.-G. Ma, "Populating ^{229}Th via two-photon electronic bridge mechanism," Nucl. Sci. Tech. **32**, 59 (2021).
[38]S. M. Brewer, J.-S. Chen, A. M. Hankin, E. R. Clements, C. W. Chou, D. J. Wineland, D. B. Hume, and D. R. Leibrandt, "^{27}Al^{+} quantum-logic clock with a systematic uncertainty below 10^{-18}," Phys. Rev. Lett. **123**, 033201 (2019).
[39]K. Beeks, T. Sikorsky, T. Schumm, J. Thielking, M. V. Okhapkin, and E. Peik, "The thorium-229 low-energy isomer and the nuclear clock," Nat. Rev. Phys. **3**, 238–248 (2021).
[40]G. E. Marti, R. B. Hutson, A. Goban, S. L. Campbell, N. Poli, and J. Ye, "Imaging optical frequencies with 100 μHz precision and 1.1 μm resolution," Phys. Rev. Lett. **120**, 103201 (2018).
[41]T. Sikorsky, J. Geist, D. Hengstler, S. Kempf, L. Gastaldo, C. Enss, C. Mokry, J. Runke, C. E. Düllmann, P. Wobrauschek, K. Beeks, V. Rosecker, J. H. Sterba, G. Kazakov, T. Schumm, and A. Fleischmann, "Measurement of the ^{229}Th isomer energy with a magnetic microcalorimeter," Phys. Rev. Lett. **125**, 142503 (2020).
[42]E. Peik and C. Tamm, "Nuclear laser spectroscopy of the 3.5 eV transition in Th-229," Europhys. Lett. **61**, 181–186 (2003).
[43]C. J. Campbell, A. G. Radnaev, A. Kuzmich, V. A. Dzuba, V. V. Flambaum, and A. Derevianko, "Single-ion nuclear clock for metrology at the 19th decimal place," Phys. Rev. Lett. **108**, 120802 (2012).
[44]L. von der Wense, B. Seiferle, M. Laatiaoui, J. B. Neumayr, H.-J. Maier, H.-F. Wirth, C. Mokry, J. Runke, K. Eberhardt, C. E. Düllmann, N. G. Trautmann, and P. G. Thirolf, "Direct detection of the ^{229}Th nuclear clock transition," Nature **533**, 47–51 (2016).
[45]J. C. Berengut, "Resonant electronic-bridge excitation of the ^{235}U nuclear transition in ions with chaotic spectra," Phys. Rev. Lett. **121**, 253002 (2018).
[46]M. A. Prelas, C. L. Weaver, M. L. Watermann, E. D. Lukosi, R. J. Schott, and D. A. Wisniewski, "A review of nuclear batteries," Prog. Nucl. Energy **75**, 117–148 (2014).
[47]Z. Movahedian and H. Tavakoli-Anbaran, "Designing a nuclear battery based on the Mo-99 radioactive source soluble in water and aqua regia in order to use in early tests," Nucl. Sci. Tech. **30**, 40 (2019).
[48]J. W. Yoon, Y. G. Kim, I. W. Choi, J. H. Sung, H. W. Lee, S. K. Lee, and C. H. Nam, "Realization of laser intensity over 10^{23} W/cm^2," Optica **8**, 630–635 (2021).
[49]P. Wang, Z. Gong, S. G. Lee, Y. Shou, Y. Geng, C. Jeon, I. J. Kim, H. W. Lee, J. W. Yoon, J. H. Sung, S. K. Lee, D. Kong, J. Liu, Z. Mei, Z. Cao, Z. Pan, I. W. Choi, X. Yan, C. H. Nam, and W. Ma, "Super-heavy ions acceleration driven by ultrashort laser pulses at ultrahigh intensity," Phys. Rev. X **11**, 021049 (2021).
[50]R. Hollinger, S. Wang, Y. Wang, A. Moreau, M. G. Capeluto, H. Song, A. Rockwood, E. Bayarsaikhan, V. Kaymak, A. Pukhov, V. N. Shlyaptsev, and J. J. Rocca, "Extreme ionization of heavy atoms in solid-density plasmas by relativistic second-harmonic laser pulses," Nat. Photonics **14**, 607 (2020).
[51]S. V. Bulanov, T. Esirkepov, and T. Tajima, "Light intensification towards the Schwinger limit," Phys. Rev. Lett. **91**, 085001 (2003).
[52]X. Zhang, J. Zhao, D. Yuan, C. Fu, J. Bao, L. Chen, J. He, L. Hou, L. Li, Y. Li *et al.*, "Deuteron-deuteron fusion in laser-driven counter-streaming collisionless plasmas," Phys. Rev. C **96**, 055801 (2017).
[53]J. Gunst, Y. Wu, N. Kumar, C. H. Keitel, and A. Pálffy, "Direct and secondary nuclear excitation with x-ray free-electron lasers," Phys. Plasmas **22**, 112706 (2015).
[54]Y.-F. He, X.-F. Xi, S.-L. Guo, B. Guo, C.-Y. He, F.-L. Liu, D. Wu, J.-H. Wei, W.-S. Yang, L.-H. Wang, D.-H. Zhang, M.-L. Qiu, G.-F. Wang, C.-Y. Li, and X.-F. Lan, "Calibration of CR-39 solid-state track detectors for study of laser-driven nuclear reactions," Nucl. Sci. Tech. **31**, 42 (2020).
[55]M. E. Foord, R. F. Heeter, P. A. M. van Hoof, R. S. Thoe, J. E. Bailey, M. E. Cuneo, H.-K. Chung, D. A. Liedahl, K. B. Fournier, G. A. Chandler, V. Jonauskas, R. Kisielius, L. P. Mix, C. Ramsbottom, P. T. Springer, F. P. Keenan, S. J. Rose, and W. H. Goldstein, "Charge-state distribution and Doppler effect in an expanding photoionized plasma," Phys. Rev. Lett. **93**, 055002 (2004).
[56]B. Manz, "Doppler shift in a plasma," J. Opt. Soc. Am. **57**, 1543–1550 (1967).
[57]J. Chihara, "Interaction of photons with plasmas and liquid metals - Photoabsorption and scattering," J. Phys.: Condens. Matter **12**, 231–247 (2000).
[58]J.-M. Chen, J.-P. Yao, Z.-X. Liu, B. Xu, F.-B. Zhang, Y.-X. Wan, W. Chu, Z.-H. Wang, L.-L. Qiao, and Y. Cheng, "Dramatic spectral broadening of ultrafast laser pulses in molecular nitrogen ions," Chin. Phys. Lett. **36**, 104204 (2019).
[59]M. Moskovits, "Surface-enhanced spectroscopy," Rev. Mod. Phys. **57**, 783–826 (1985).